Unstructured, anisotropic mesh generation for the Northwestern European continental shelf, the continental slope and the neighbouring ocean

Sébastien Legrand [a,b], Eric Deleersnijder [a,b,1], Eric Delhez [c] and Vincent Legat [b]

[a] *G. Lemaître Institute of Astronomy and Geophysics, Université catholique de Louvain. 2, Chemin du Cyclotron. B-1348 Louvain-la-Neuve, Belgium.*

[b] *Centre for Systems Engineering and Applied Mechanics, Université catholique de Louvain. 4, Avenue Georges Lemaître. B-1348 Louvain-la-Neuve, Belgium.*

[c] *Modélisation et Méthodes Mathématiques, Université de Liège. Sart Tilman B37, B-4000 Liège, Belgium.*

Abstract

A new mesh refinement strategy for generating high quality unstructured meshes of the Northwestern European continental shelf, the continental slope and the neighbouring ocean is presented. Our objective is to demonstrate the ability of anisotropic unstructured meshes to adequately address the challenge of simulating the hydrodynamics occurring in these three regions within a unique mesh. The refinement criteria blend several hydrodynamic considerations as the tidal wave propagation on the continental shelf and the hydrostatic consistency condition in steep areas. Several meshes illustrate both the validity and the efficiency of the refinement strategy. The selection of the refinement parameters is discussed. Finally, an attempt is made to take into account tidal ellipses, providing another cause for anisotropy in the mesh.

Key words: Unstructured grids, Northwestern European continental shelf, Delaunay triangulation, Finite elements methods, Finite volumes methods

[1] Corresponding author — *Email address:* ericd@uclouvain.be

Revised version submitted to Continental Shelf Research *24 May 2007*

1 Introduction

During the last decade, the focus in shelf oceanography moved from the shelf itself to more coastal areas, on the one side, and to the shelf break region, on the other side. In particular, recognizing the major influence of the exchanges between the shelf and the deep ocean on the climate, the primary productivity and many pollution issues of shelf seas (Walsh, 1991), numerous research programs were initiated to describe, understand and quantify the fluxes across the shelf break. Those include ECOMARGE, MORENA, ARCANE, OMEX, SEFOS, SES, ENAM II, SEEP I and II or CODE7. The European Union's Ocean Margin EXchange (OMEX) studied carbon and nitrogen distributions and fluxes on the Northwestern European continental shelf margin and slope (Wollast and Chou, 2001). The UK Natural Environment Research Council (NERC) Land Ocean-Interaction Study (LOIS) Shelf Edge Study (LOIS-SES) aimed at the quantification of the contributions to ocean-shelf water exchange by physical processes in the shelf-edge region west of Scotland (Souza et al., 2001). The resulting analysis provided the background of more environmental oriented studies in which fluxes of dissolved and suspended sediments were estimated. Similar projects like the Shelf Edge Exchange Processes studies (SEEP-I, SEEP-II) focused on the Middle Atlantic Bight of the eastern U.S. continental shelf and slope (Walsh et al., 1988; Biscaye et al., 1994).

Extended measurement campaigns in shelf break regions are always severely constrained by the weather and their significance is also difficult to assess because of the high spatial and temporal variability of the hydrodynamics of these regions. The same high level of variability and the large number of interacting processes make the numerical approach also very challenging. In order to estimate the fluxes between the deep ocean and the shelf, a model must not only be able to describe the hydrodynamics of both regions but also manage to capture the physics of the shelf break region (Huthnance, 1995) : complex bathymetry, intensification of tidal currents near the shelf edge, non-linear interactions with the steep topography and the density structure, wind induced upwelling of deep cold water in a bottom boundary layer with enhanced mixing over the shelf or downwelling of light surface water with rapid vertical mixing, formation and instabilities of shelf-edge fronts, generation of internal tides and associated turbulence energy and mixing, etc. Davies and Xing (2005) present a review of these processes that influence the exchange between ocean and shelf.

Candidate models must not only be fully non-linear but also provide a very high spatial resolution for the accurate description of the complex hydrodynamics in the shelf break region. Coelho et al. (2002), using a 8.5 km horizontal resolution model of the west coasts of Iberia and Morocco, stress that the use of high resolution implies a limited extent model for which bound-

ary conditions are difficult to assess. The usual approach is therefore to use high-resolution process models of the shelf break region or nested models with increased resolution at the shelf break. In the LOIS Shelf Edge Study project, for instance, a 3-D hydrodynamic model with grid resolution $(1/24)^\circ \times (1/24)^\circ$ was used to study spatial variability of the tides and wind-driven circulation west of Scotland (Xing and Davies, 1998b). The model was used in the form of a cross-shelf section with finer resolution (about 1 km or less) to examine the generation of internal tides (Xing and Davies, 1997), the dynamics of suspended sediments (Xing and Davies, 1998a), small scale mixing (Davies and Xing, 2002) and tidal rectification and other non-linear processes (Davies and Xing, 2003). Finally, a 2-D model of the cross-slope section was run for a seasonal cycle of stratification with tidal, wind and thermal forcing (Xing et al., 1999). Microbiological models were incorporated to model the primary production cycle in conjunction with physics and SPM transports (Proctor et al., 2003). Non-hydrostatic models have been used to study the the generation of internal tides and their non-linear interaction with the topography (Lamb, 1994, 2004; Legg, 2004a,b).

Most current models of the large-scale ocean circulation encompass (part of) the adjacent shelf regions. Similarly, the open boundary of most shelf models has been moved from the shelf break itself to deeper areas. The aim of such expansion of the geographic extent is generally to provide more appropriate boundary conditions (Gerritsen et al., 1995; Skogen et al., 1995). In some model systems, a nesting approach is used with large-scale ocean models providing boundary conditions to force fine resolution model of the shelf or part of it. In the so-called 'Atlantic-Margin' configuration of the POLCOMS model system (Holt et al., 2005), for instance, the western boundary of the shelf model is located in the deep ocean and the boundary data are obtained from the U.K. Meteorological Office Forecasting Ocean Assimilation Model — FOAM — (Bell et al., 2000). Higher resolution nested models are also included to describe specific parts of the Northwestern European Continental Shelf (Holt et al., 2004). Multiscale modelling exercises are planned in which the output of the large scale MERCATOR ocean model systems are used to force coastal models (Chanut and Etienne, 2005). Lynch et al. (2003 and 2004) model the hydrodynamics of the Western Irish Sea region with their QUODDY finite element model using a graded mesh of triangles with 5 discrete levels of resolution increasing from 0.02° at the Irish coast to 0.32° in the shelf break region and in the deep ocean. Such a nesting approach is only partly satisfactory. While an increased resolution is provided in the area of interest — part of the shelf region — and larger scales influences from the adjacent ocean are taken into account in some way in the local model, the dynamics of the shelf break region is generally poorly represented. As a consequence, the exchange processes between the shelf and the deep ocean are not properly described.

An alternative approach is the use of unstructured meshes that easily allow

within the same mesh local refinement along the shelf break while covering the oceanic and shelf domains at an appropriate resolution. Indeed, as unstructured mesh marine modelling is a rapidly growing field of research (Hanert et al., 2005; Walters, 2005; Pietrzak et al., 2005; Pain et al., 2005), it is now conceivable to develop an unstructured mesh numerical simulation tool of the Northwestern European continental shelf, the continental slope and the neighbouring ocean. In this perspective, Hall and Davies (2005) have compared the results of an unstructured mesh finite element model (QUODDY) with those of a finite difference one (Xing and Davies, 1998b) on the Malin-Hebrides shelf. This intercomparison suggests that the finite element model with a refined mesh in the shelf break region is more accurate in generating and propagating the internal tide than the finite difference model.

The present article deals with the first step towards the development of such a model, i.e. the construction of an appropriate mesh for the Northwestern European continental shelf and a part of the North Atlantic Ocean (Figure 1). As the small aspect ratio of most marine flows suggests to explicitly preserve the vertical direction in the mesh, we have chosen to use *prismatic elements* that may be obtained from a downwards extrusion of a surface triangulation. This allows to treat separately the horizontal triangulation at the surface and the positioning of the nodes along each vertical. Otherwise stated, the quadrangular faces of the prismatic elements are aligned with the vertical direction while the triangular ones can be directed according to some criteria for reaching a situation analogous to the generalised vertical coordinates (Kasahara, 1974; Thompson et al., 1985; Deleersnijder and Ruddick, 1992; Adcroft and Hallberg, 2004). Those are mainly similar to the terrain-following $\sigma-$coordinates close to the seabed and at the shelf break. Only the problem of a surface triangulation generation is addressed herein.

Since generating triangulation is very well documented in the literature (Watson, 1981; Bowyer, 1981; Frey, 1987; Shewchuk, 1996; Frey and George, 2000; Legrand et al., 2000), the challenge consists in the design of a suitable mesh refinement strategy. This task is crucial in order for the model to take advantage of all of the aspects of unstructured meshes. As mesh refinement results from the consideration of many constraints, setting up a feasible unstructured mesh refinement strategy is a non-trivial task. This should be guided by the major physical processes occurring along the shelf break and on the continental shelf. Since tides are among the most energetic processes occurring on the continental shelf and control to a large extent the level of bottom friction and background turbulence on the shelf and at the shelf edge, their accurate simulation is prerequisite for the reliable modelling of other processes. The tidal dynamics must therefore be taken into account in the mesh generation algorithm. Similarly, the strong and narrow slope current that flows from the Bay of Biscay to the Norwegian Trench suggests the introduction of some anisotropy along the shelf break. However, physical considerations are

not the only constraints on the mesh generation procedure: the hydrostatic consistency criterion has also to be considered at the shelf break in order to limit the error on the pressure gradient term inherent in generalised vertical coordinates (e.g. Haney 1991; Deleersnijder and Beckers 1992; Shchepetkin and McWilliams, 2003). This criterion relates the horizontal and the vertical resolution. Section 2 details our refinement strategy. Section 3 introduces two gauges to evaluate the quality of the Northwestern European continental shelf triangulations that are presented in section 4. Finally, concluding remarks are given.

2 A refinement strategy for the Northwestern European continental shelf

A mesh generator is a tool that takes into account constraints on the size, the shape and the orientation of the elements making up a triangulation of the domain of interest. It is assumed that the ideal mesh is composed of unitary equilateral triangles in a dual space where the modified coordinates $\mathbf{x}'$ are obtained from the transformation of the coordinates $\mathbf{x}$ in the physical space: $\mathbf{x}' = \mathbf{f}(\mathbf{x})$. This transformation is characterized by the metric tensor $\mathbf{g}(\mathbf{x})$ that relates length between both spaces:

$$\mathrm{d}\mathbf{x}' \cdot \mathrm{d}\mathbf{x}' = \mathrm{d}\mathbf{x} \cdot \mathbf{g}(\mathbf{x}) \cdot \mathrm{d}\mathbf{x}. \tag{1}$$

The length of a curve Γ in the physical space and the dual space are thus respectively given by

$$l = \int_{\Gamma} \sqrt{\mathrm{d}\mathbf{x} \cdot \mathrm{d}\mathbf{x}}$$

$$l' = \int_{\Gamma} \sqrt{\mathrm{d}\mathbf{x}' \cdot \mathrm{d}\mathbf{x}'} = \int_{\Gamma} \sqrt{\mathrm{d}\mathbf{x} \cdot \mathbf{g}(\mathbf{x}) \cdot \mathrm{d}\mathbf{x}}.$$

In this framework, the goal of the mesh generator consists in creating a mesh with all edges exhibiting a length in the dual space as close as possible to unity. To reach such a goal, vertices can be created, removed or displaced. Topological operations like edge flipping or re-performing a partial Delaunay triangulation can also be done (Legrand et al., 2000). Of course, the suitable metric $\mathbf{g}(\mathbf{x})$ needs to be available.

To adequately build up a metric for a two-dimensional domain, only three parameters have to be provided. Those are the *privileged direction* — i.e. a unit

vector (v_x, v_y) — along which the element should be elongated and two *target element size* function $h_{//}(\mathbf{x})$ and $h_{\perp}(\mathbf{x})$ that set the element length along the privileged direction (v_x, v_y) and the normal direction $(-v_y, v_x)$, respectively. Those three parameters fully determine the orthonormal eigenvectors and eigenvalues of the metric tensor:

$$\begin{aligned}\mathbf{g}(\mathbf{x}) &= \begin{pmatrix} v_x(\mathbf{x}) & -v_y(\mathbf{x}) \\ v_y(\mathbf{x}) & v_x(\mathbf{x}) \end{pmatrix} \begin{pmatrix} \dfrac{1}{h_{//}^2(\mathbf{x})} & 0 \\ 0 & \dfrac{1}{h_{\perp}^2(\mathbf{x})} \end{pmatrix} \begin{pmatrix} v_x(\mathbf{x}) & v_y(\mathbf{x}) \\ -v_y(\mathbf{x}) & v_x(\mathbf{x}) \end{pmatrix} \\ &= \begin{pmatrix} \dfrac{v_x^2}{h_{//}^2} + \dfrac{v_y^2}{h_{\perp}^2} & \dfrac{v_x v_y}{h_{//}^2} - \dfrac{v_x v_y}{h_{\perp}^2} \\ \dfrac{v_x v_y}{h_{//}^2} - \dfrac{v_x v_y}{h_{\perp}^2} & \dfrac{v_y^2}{h_{//}^2} + \dfrac{v_x^2}{h_{\perp}^2} \end{pmatrix}. \end{aligned} \tag{2}$$

Thus, setting up a mesh refinement strategy is tantamount to suggesting a method for evaluating the parameters $h_{\perp}$, $h_{//}$ and (v_x, v_y) at any location in the domain of interest. This will be done by taking into account some aspects of the physics of tidal propagation and a numerical accuracy constraint related to the evaluation of the pressure gradient in regions where the seabed exhibits steep slopes (e.g. Haney 1991, Deleersnijder and Beckers 1992), i.e. essentially the shelf break and the continental slope.

2.1 Tidal propagation

Tides are the most energetic processes occurring on the Northwestern European continental shelf. As Henry and Walters (1993), Foreman et al. (1995), Hagen et al. (2001), Jarosz et al. (2005), Walters (2005) or Legrand et al. (2006), we may therefore assume that the resolution of an appropriate mesh should be adjusted in such a way that external inertia-gravity waves travel over a given time interval roughly the same fraction of the mesh elements. Since the tide celerity is approximately given by $\sqrt{g\ D(\mathbf{x})}$ — where g and $D(\mathbf{x})$ are the gravitational acceleration and the water column depth, respectively — such a requirement can be expressed as

$$\frac{h_{//}(\mathbf{x})}{h^*} = \sqrt{\frac{D(\mathbf{x})}{D^*}}. \tag{3}$$

This relation specifies the target element size $h_{//}(\mathbf{x})$ in terms of the water column depth field $D(\mathbf{x})$ and a user specified target element size h^* for a

given water column depth D^*. This strategy tends to produce fine elements in the shallowest parts of the domain of interest and the coarsest elements in deeper area.

As no privileged direction was specified, expression (3) introduces no anisotropy in the mesh: $h_\perp(\mathbf{x})$ should be equal to $h_{//}(\mathbf{x})$. However, anisotropy is necessary in steep regions, as is explained below.

2.2 Shelf break and continental slope

Narrow slope currents flowing along the shelf break and internal tides generation are typical examples of the shelf break dynamics. These are both very sensitive to current profile, bathymetry and stratification. For instance, the latter is critically dependent upon the bathymetry gradient component normal to the flow of the barotropic tidal energy while the former tends to follow geostrophic contours (Huthnance, 1995). Therefore, their accurate modelling requires to resolve both the details of the bottom topography and the forces driving the flow. In particular, the discretisation of the internal pressure gradient is no trivial task in regions characterised by steep slopes of the seabed.

A first strategy for refining the mesh in the region of the shelf break may be based on the Hessian matrix of the water column depth (Gorman et al., 2005). However, this approach aims at uniformly distributing over the mesh the discretisation errors associated with the water column depth and is not directly related to hydrodynamic processes. This is the reason why we prefer to adopt a strategy that is explicitly based on errors due to the discretisation of some critical terms of the momentum equations. For a region of steep bottom slopes, the hydrostatic consistency condition is the refinement criterion of choice, provided the discretisation in the vertical direction bears similarities with the terrain-following σ-coordinate system ($\sigma = 0$ at the seabed and $\sigma = 1$ at the sea surface). In the notations of the present study, this condition,

$$\left|\left|\frac{1-\sigma}{D(\mathbf{x})}\boldsymbol{\nabla} D(\mathbf{x})\right|\right| h_\perp(\mathbf{x}) < \delta\sigma, \tag{4}$$

requires a sufficiently small element size in the direction of the depth gradient for a given vertical grid increment $\delta\sigma$ for the error on the numerical estimate of the internal pressure gradient to be small in the direction orthogonal to the isobaths (Janjic, 1977; Mesinger, 1982; Haney, 1991; Deleersnijder and Beckers, 1992; Beckmann and Haidvogel, 1993; Shchepetkin and McWilliams, 2003). Since the hydrostatic consistency condition is the most stringent at the seabed, we define the target element size along the depth gradient direction

as

$$h_\perp(\mathbf{x}) = s \left|\left| \frac{\boldsymbol{\nabla} D(\mathbf{x})}{D(\mathbf{x})} \right|\right|^{-1} . \tag{5}$$

The value of the user specified parameter s must be smaller than the vertical increment $\delta\sigma$ at the seabed. Actually, even if numerical considerations motivate relation (5), the horizontal length scale $\left|\left| \frac{\boldsymbol{\nabla} D(\mathbf{x})}{D(\mathbf{x})} \right|\right|^{-1}$ appears in every analytical study of the shelf break dynamics (Huthnance, 1995) and is also the relevant parameter for the generation of internal tides (Xing and Davies, 1998b).

2.3 Building the metric tensor

Based on the considerations above, the metric tensor will be built as illustrated in Figure 2. The following steps are performed:

- The privileged direction (v_x, v_y) is set along the direction normal to the bathymetry gradient. In case of no privileged direction — no gradient — the mesh refinement strategy should be isotropic: $h_{//}$ is equal to $h_\perp$ such that, according to (2), the privileged direction can be set to an arbitrary value.
- From bathymetric data, the speed of external gravity waves, i.e. $\sqrt{g\ D}$, is evaluated in the domain of interest. Using (3), this leads to a first estimate of the mesh size target $h_{//}$. However, this strategy can lead to excessively small elements in the shallowest coastal areas or to excessively large elements in the open ocean. The latter decrease the model accuracy while the former can prohibitively increase the computational cost. This is why $h_{//}$ must be forced to remain between minimum (h_{min}) and maximum (h_{max}) values set a priori. In other words, the mesh size target $h_{//}$ is prescribed as

$$h_{//} = \max\left[h_{min}, \min\left(h_{max}, h^* \sqrt{\frac{D(\mathbf{x})}{D^*}}\right)\right] . \tag{6}$$

- Using expression (5), $h_\perp$ is estimated as

$$h_\perp = \min\left[h_{//}(\mathbf{x}), s \left|\left| \frac{\boldsymbol{\nabla} D(\mathbf{x})}{D(\mathbf{x})} \right|\right|^{-1}\right] . \tag{7}$$

This simple definition works out the compromise between the assumed requirement of isotropy on the shelf and the possible need of anisotropy for accurately modelling the shelf break dynamics.

So, if the bathymetric gradient is small, the mesh size targets $h_{//}$ and $h_{\perp}$ will be equal; otherwise, $h_{\perp}$ will be set to a value smaller than $h_{//}$ and the mesh will tend to exhibit an appropriate degree of anisotropy. As shown in Figure 3, anisotropic elements are likely to be generated at the shelf margin, along the coastlines and close to the steepest seamounts.

3 Gauges to evaluate the mesh quality

The role of the mesh generator is to create the grid that provides the best numerical accuracy for a given number of degrees of freedoms. Basically, the target element size requirement has to be satisfied along with two other important constraints. For most discretisation techniques like finite volumes or finite elements, it is necessary to avoid large local discrepancies in element sizes. The second key-point is to estimate element equilaterality in the suitable metric. In this section, we define two quality gauges to analyze the geometrical quality of our generated meshes: a *shape gauge* and an *edge gauge* (Legrand et al., 2006).

Following Dompierre et al. (2003), the local shape measure of an element Ω^e is given by a normalized dimensionless *shape gauge* β_e:

$$\beta_e = \frac{\sqrt{3\ b^e \prod_{i=1}^{3} (b^e - 2\ b_i^e)}}{\left(b^e \ \max_i \ b_i^e \right)} \quad , \tag{8}$$

where b_i^e and $b^e = b_1^e + b_2^e + b_3^e$ are the lengths of the edges Γ_i^e of the element Ω^e and its perimeter in the dual space :

$$b_i^e = \int_{\Gamma_i^e} \sqrt{\mathrm{d}\mathbf{x} \cdot \mathbf{g}(\mathbf{x}) \cdot \mathrm{d}\mathbf{x}}. \tag{9}$$

This gauge can be viewed as a normalized ratio of the radius of the inscribed circle of the triangular element Ω^e in the dual space with respect to its perimeter. The normalization ensures that the shape gauge lies in the interval $[0, 1]$ and is maximal for the ideal case: an equilateral triangle in the dual space or, equivalently, an anisotropic triangle whose shape and orientation in the physical space exactly fulfill the metric tensor constraints.

As the shape gauge does not give any piece of information about the size of the elements, we introduce a second quality gauge that measures the discrepancy

between the target length (1 in the dual space) and the length of an edge Γ_f. This *edge gauge* γ_f, defined as

$$\gamma_f = 1 - |b_f - 1|, \tag{10}$$

is maximal for the ideal case: $b_f = 1$, i.e. when the obtained length is in perfect agreement with the target element size fields.

Finally, two global quality indexes β and γ may be defined as the mean values of both gauges β_e and γ_f over the whole mesh, respectively.

4 Results

The methodology and the gauges introduced above are now used for generating and assessing anisotropic unstructured meshes for the Northwestern European continental shelf, the continental slope and the neighbouring ocean in an automatic way using our own implementation of the Watson-Bowyer algorithm (Legrand et al., 2000). Although the geographical domain spreads from $20°W$ to $13°E$ and from $43°N$ to $63°N$, UTM coordinates have been used in order to easily evaluate lengths in the international metric system. The bathymetry gradients and the coastlines description have been obtained from the ETOPO-5 gridded dataset (National Geophysical Data Center, 1988).

Figure 4 illustrates the ability of our mesh refinement strategy to adequately resolve the continental shelf, the shelf break and the seamounts. The design parameters are summarized in Table 1. For this first 'coarse' example, the element size ranges from 6 km in the nearshore region to about 40 km in the open ocean. Element size variation in terms of the square root of the water depth may clearly be noticed on the continental shelf. The close-up view on the Hebridean shelf shows that the anisotropy is mainly confined along the shelf break and the seamounts. The minimal transverse element size $h_\perp$ is about 3 km at the shelf break. The anisotropy factor $r = h_{//}/h_\perp$ varies according to the local values of the target element sizes $h_{//}$ and $h_\perp$. Its maximal value is about 10. Another advantage of the unstructured meshes is their ability to resolve islands, channels and shorelines without introducing any 'staircase' discretisation. The latter, as is well known, are likely to cause spurious coastal boundary layers (Davies and Jones, 1996; Adcroft and Marshall, 1998) that can limit the model accuracy in coastal areas.

Figure 5 shows the way our mesh generator can fulfill the mesh refinement strategy under quality constraints. The first column refers to the coarse mesh presented in Figure 4. That the mean values of the shape gauge ($\beta = 0.83$) and the edge gauges ($\gamma = 0.87$) are rather close to unity indicates that the

generated mesh is in a good agreement with the metric tensor prescriptions in most regions of the domain of interest. However, some discrepancies with those prescriptions can locally arise in regions where the topographic features are not adequately resolved as the narrow passage between the Anton Dohrn seamount and the Hebridean shelf. These regions can be brought to the fore by graphically comparing the length, the shape and the orientation of the generated elements with ellipses that delimit regions laying at a distance of 1/2 in the dual space from mesh vertices: overlapping ellipses in the narrow passage indicates the poor quality elements. These increase the length of the tail of both quality gauges normalized distributions to an unacceptable limit.

The second column of Figure 5 presents results with another set of the design parameters values (Table 1). These have been chosen according to recommendations in Xing et al. (1999): a transverse element size $h_\perp$ of about 0.5 km in the steepest areas of the shelf break and a vertical increment $\delta\sigma$ at the seabed of a few hundredth ($s = 0.05$). The nearshore region is covered with elements of 0.5 km in length while the length of the elements in the open ocean is of order 5 km. These design parameters values allow a better resolution of the topographic features leading to a better quality mesh. In particular, the fine mesh does not have overlapping ellipses while the tails of both gauges normalized distribution are drastically shortened: the worst values for both quality gauges are greater than 0.5. Finally, it must be pointed out that the 1.7 millions of elements contained in this fine mesh is still a quite small number in comparison with the 12.4 millions of squares needed to cover the whole domain (3.1 10^6 km^2) with a uniform structured grid whose elements edges present the same typical size, i.e. 0.5 km.

5 Concluding remarks

This paper presents the potential advantages of anisotropic unstructured meshes for modelling the hydrodynamics of the Northwestern European continental shelf, the continental slope and the neighbouring ocean within the same mesh. Taking advantages of the knowledge of the dynamics of the three parts of the domain, we have developed a simple but efficient strategy in which the mesh refinement is controlled through a few design parameters. The analyses of the quality of the generated meshes demonstrate that, while major topographic features are correctly resolved in both the along-slope and the cross-slope directions, anisotropic graded meshes can be obtained with good geometrical properties. The latter ensure a good numerical conditioning for finite element or finite volume hydrodynamic models. However, only numerical simulations can fully validate the usefulness of the strategy. Those will be performed with the forthcoming SLIM-3D baroclinic model (http://www.astr.ucl.ac.be/SLIM/).

Our mesh refinement strategy is both relatively simple and efficient. While primarily designed here to ensure appropriate description of the most energetic shelf and shelf edge processes, it can also easily be extended to cope with other processes as internal tide, secondary along shelf processes, coastal dynamics or tidal front processes. Let us give two attractive examples. First, the accurate simulation of small-scale details of pollutants transport could require the enhancement of the nearshore resolution by blending our mesh refinement strategy with other constraints based on the distance to the shore (Legrand et al., 2006). However, this cannot be envisaged without using the finest bathymetry data, the finest coastlines description and a suitable wetting and drying procedure. A second potential improvement could be the exploitation of tidal ellipses in order to introduce some anisotropy on the continental shelf. For instance, to take into account the fact that the flows are mainly oriented along narrow channels as the North Channel or the Saint George's Channel in the Irish sea, the privileged directions of Figure 6 are given by the M_2 tide ellipses (Luyten et al., 1999); the mesh size $h_{//}$ by relation (6) and finally, the anisotropy factor $r = h_{//}/h_{\perp}$ by an adequate fraction of the ratio between the semi-axis of these tidal ellipses. Although this seems very attractive, no claim can be made at this stage that this will improve the simulations accuracy. However, it illustrates a way to extend our approach to dynamically adjusted meshes.

Acknowledgements

Eric Deleersnijder is a Research Associate with the Belgian National Fund for Scientific Research (FNRS). The present study was carried out within the scope of the project "A second-generation model of the ocean system", which is funded by the *Communauté Française de Belgique*, as *Actions de Recherche Concertées*, under contract ARC 04/09-316. This work is a contribution to the development of SLIM, the Second-generation Louvain-la-Neuve Ice-ocean Model. The authors are indebted to Georges Pichot and Virginie Pison for providing tidal currents time-series computed with COHERENS (Luyten et al., 1999).

References

Adcroft, A., Hallberg, R., 2004. On methods for solving the oceanic equations of motion in generalized vertical coordinates. Ocean Modelling 11, 224–233.

Adcroft, A., Marshall, D., 1998. How slippery are piecewise-constant coastlines in numerical models? Tellus 50 A, 95–108.

Beckmann, A., Haidvogel, D., 1993. Numerical simulation of flow around a tall

isolated seamount. part I: problem formulation and model accuracy. Journal of Physical Oceanography 23, 1736–1753.

Bell, M.J., Forbes, R.M., Hines, A., 2000. Assessment of the FOAM global data assimilation system for real-time operational ocean forecasting. Journal of Marine Systems 25, 1–22.

Biscaye, P.E., Flagg, C.N., Falkowski, P.G., 1994. The shelf edge exchange processes experiment, SEEP-II: an introduction to hypotheses, results and conclusions. Deep Sea Research II 41, 231–252.

Bowyer, A., 1981. Computing Dirichlet tesselations. The Computer Journal 24 (2), 162–167.

Chanut, J., Etienne, H., 2005. Forcing coastal model with MERCATOR data. Mercator Ocean Quarterly Newsletter 18, 2–3.

Coelho, H.S., Neves, R.J.J., White, M., Leito, P.C., Santos, A.J., 2002. A model for ocean circulation on the Iberian coast. Journal of Marine Systems 32 (1-3), 153–179.

Davies, A.M., Jones, J.E., 1996. Sensitivity of tidal bed stress distributions, near-bed currents, overtides, and tidal residuals to frictional effects in the eastern irish sea. Journal of Physical Oceanography 26, 2553–2575.

Davies, A.M., Xing, J., 2002. Processes influencing sediment movement on the Malin-Hebrides shelf. Continental Shelf Research 22, 2081–2113.

Davies, A.M., Xing, J., 2003. On the interaction between internal tides and wind induced near inertial currents at the shelf edge. Journal of Geophysical Research 108(C3), 3099.

Davies, A.M., Xing, J., 2005. Modelling process influencing shelf edge exchange of water and suspended sediment. Continental Shelf Research 25, 973–1001.

Deleersnijder, E., Beckers, J.-M., 1992. On the use of σ-coordinate in regions of large bathymetric variations. Journal of Marine Systems 3, 381–390.

Deleersnijder, E., Ruddick, K.G., 1992. A generalized vertical coordinate for 3D marine models. Bulletin de la Société Royale des Sciences de Liège 61 (6), 489–502.

Dompierre, J., Vallet, M.-G., Labb, P., Guibault, F., 2003. On simplex shape measures with extension for anisotropic meshes. In: Workshop on mesh quality and dynamic meshing. Sandia National Laboratories - Livermore, CA, pp. 46–71.

Foreman, M.G.G., Walters, R.A., Henry, R.F., Keller, C.P., Dolling, A.G., 1995. A tidal model for eastern Juan de Fuca Strait and the southern Strait of Georgia. Journal of Geophysical Research 100 (C1), 721–740.

Frey, P., George, P., 2000. Mesh generation : Application to finite elements. Hermes Science Publishing.

Frey, W., 1987. Selective refinement: A new strategy for automatic node placement in graded triangular meshes. International Journal for Numerical Methods in Engineering 24 (11), 2183–2200.

Gerritsen, H., de Vries, j.W., Philippart, M.E., 1995. The dutch continental shelf model. Quantitative Skill Assessment for Coastal Ocean Models, Coastal and Estuarine Studies 48, 425–467.

Gorman, G.J., Piggott, M.D., Pain, C.C., de Oliveira, C.R.E., Umpleby, A.P., Goddard, A.J.H., 2005. Optimisation based bathymetry approximation through constrained unstructured mesh adaptivity. Ocean Modelling accepted for publication.

Hagen, S.C., Westerink, J.J., Kolar, R.L., Horstmann, O., 2001. Two-dimensional, unstructured mesh generation for tidal models. International Journal for Numerical Methods in Fluids 35, 669–686.

Hall, P., Davies, A.M., 2005. Comparison of finite difference and element models of internal tides on the malin-hebrides shelf. Ocean Dynamics 55, 272–293.

Hanert, E., Le Roux, D.Y., Legat, V., Deleersnijder, E., 2005. An efficient Eulerian finite element for the shallow water equations. Ocean Modelling 10, 115–136.

Haney, R.L., 1991. On the pressure gradient force over steep topography in sigma coordinate ocean models. Journal of Physical Oceanography 21, 610–619.

Henry, R., Walters, R., 1993. Geometrically based, automatic generator for irregular networks. Communications in Numerical Methods in engineering 9, 555–566.

Holt, J.T., Allen, J.I., Proctor, R., Gilbert, F., 2005. Error quantification of a high-resolution coupled hydrodynamic-ecosystem coastal-ocean model: Part 1 model overview and assessment of the hydrodynamics. Journal of Marine Systems 57 (1-2), 167–188.

Holt, J.T., Proctor, R., Blackford, J.C., Allen, J.I.., Ashworth, M., 2004. Advective controls on primary production in the stratified western Irish Sea: an eddy-resolving model study. Journal of Geophysical Research 109, 5024.

Huthnance, J.M., 1995. Circulation, exchange and water masses at the ocean margin: the role of physical processes at the shelf edge. Progress in Oceanography 35, 353–431.

Janjic, Z.I., 1977. Pressure gradient force and advection scheme used for forecasting with steep and small scale topography. Contributions to Atmospheric Physics 50, 186–199.

Jarosz, E., Blain, C.A., Murray, S.P., Inoue, M., 2005. Barotropic tides in the Bab el Mandab Straits — numerical simulations. Continental Shelf Research 25, 1225–1247.

Kasahara, A., 1974. Various vertical coordinate systems used for numerical weather predictions. Monthly Weather Review 102, 509–522.

Lamb, K.G., 1994. Numerical experiments of internal wave generation by strong tidal flow across a finite amplitude bank edge. Journal of Geophysical Research 99 (C1), 843–864.

Lamb, K.G., 2004. Nonlinear interaction among internal wave beams generated by tidal flow over supercritical topography. Geophysical Research Letters 31 (L09313), doi:10.1029/2003GL019393.

Legg, S., 2004a. Internal tides generated on a corrugated continental slope. Part I: cross-slope barotropic forcing. Journal of Physical Oceanography

34, 156–173.

Legg, S., 2004b. Internal tides generated on a corrugated continental slope. Part II: along-slope barotropic forcing. Journal of Physical Oceanography 34, 1824–1838.

Legrand, S., Deleersnijder, E., Hanert, E., Legat, V., Wolanski, E., 2006. High-resolution, unstructured meshes for hydrodynamic models of the Great Barrier Reef, Australia. Estuarine, Coastal and Shelf Sciences in press.

Legrand, S., Legat, V., Deleersnijder, E., 2000. Delaunay mesh generation for an unstructured-grid ocean general circulation model. Ocean Modelling 2, 17–28.

Luyten, P.J., Jones, J.E., Proctor, R., Tabor, A., Tett, P., Wild-Allen, K., 1999. Coherens - a coupled hydrodynamical-ecological model for regional and shelf seas: User documentation. Mumm report, Management Unit of the Mathematical Models of the North Sea.

Lynch, D.R., Naimie, C.E., Smith, K.W., 2003. Tidal atlas for the Irish Shelf Seas. Numerical Methods Laboratory Report NML-03-7, Dartmouth College, Hanover NH USA.

Lynch, D.R., Smith, K.W., Cahill, B., 2004. Seasonal mean circulation on the Irish shelf a model-generated climatology. Continental Shelf Research 24, 2215–2244.

Mesinger, F., 1982. On the convergence and error problems of the calculation of the pressure gradient force in sigma coordinate models. Geophysical, Astrophysical Fluid Dynamics 19, 105–117.

National Geophysical Data Center, 1988. Digital relief of the surface of the earth. Tech. Rep. Data Announcement 88-MGG-02, NOAA, Boulder.

Pain, C.C., Piggott, M.D., Goddard, A.J.H., Fang, F., Gorman, G.J., Marshall, D.P., Eaton, M.D., Power, P.W., de Oliveira, C.R.E., 2005. Three-dimensional unstructured mesh ocean modelling. Ocean Modelling 10 (1-2), 5–33.

Pietrzak, J., Deleersnijder, E., Schroeter, J. (Eds.), 2005. The Second International Workshop on Unstructured Mesh Numerical Modelling of Coastal, Shelf and Ocean Flows. Ocean Modelling (special issue) 10 (1-2), 1-252.

Proctor, R., Chen, F., Tett, P.B., 2003. Carbon and nitrogen fluxes across the Hebridean shelf break, estimated by 2D coupled physical-microbiological model. The Sciences of the Total Environment 314-316, 787–800.

Shchepetkin, A.F., McWilliams, J.C., 2003. A method for computing horizontal pressure-gradient force in an oceanic model with a nonaligned vertical coordinate. Journal of Geophysical Research 108 (C3), 3090.

Shewchuk, J.R., 1996. Triangle: Engineering a 2d quality mesh generator and delaunay triangulator. In: First Workshop on Applied Computational Geometry (Philadelphia, Pennsylvania). Association for Computing Machinery, pp. 124–133.

Skogen, M. D., Svendsen, E., Berntsen, J., Aksnes, D.L., Ulvestad, K.B., 1995. Modelling the primary production in the North Sea using a coupled 3-dimensional physical chemical biological ocean model. Estuarine, Coastal

and Shelf Sciences 41, 545–565.

Souza, A.J., Simpson, J.H., Harikrishnan, M., Malarkey, J., 2001. Flow structure and seasonability in the Hebridean slope current. Oceanol Acta 24, S63–S76.

Thompson, J.F., Warsi, Z.U.A., Mastin, C.W., 1985. Numerical Grid Generation. Foundations and applications. North Holland.

Walsh, J.J., 1991. Importance of continental margins in the marine biogeochemical cycling of carbon and nitrogen. Nature 350 (6313), 53–55.

Walsh, J.J., Biscaye, P.E., Csanady, G.T., 1988. The 1983-1984 Shelf Edge Exchange Processes (Seep)-I: hypotheses and highlights. Continental Shelf Research 8, 435–456.

Walters, R., 2005. Coastal ocean models: Two useful finite element methods. Continental Shelf Research 25, 775–793.

Watson, D., 1981. Computing the n-dimensional Delaunay tesselation with applications to Voronoi polytopes. The Computer Journal 24 (2), 167–172.

Wollast, R., Chou, L., 2001. Ocean Margin Exchange in the Northern Gulf of Biscay: OMEX I an introduction. Deep Sea Research II 48 (14/15), 2971–2978.

Xing, J., Chen, F., Proctor, R., 1999. A two-dimensional slice model of the shelf edge region off the west coast of Scotland: model response to realistic seasonal forcing and the role of M2 tide. Continental Shelf Research 19 (10), 1353–1386.

Xing, J., Davies, A.M., 1997. The influence of wind effects upon internal tides in the shelf edge regions. Journal of Physical Oceanography 27, 2100–2125.

Xing, J., Davies, A.M., 1998a. Formulation of a three-dimensional shelf edge model and its application to inertial tide generation. Continental Shelf Research 18 (2-4), 405–440.

Xing, J., Davies, A.M., 1998b. A three-dimensional model of internal tides on the malin-hebrides shelf and shelf edge. Journal of Geophysical Research 103 (C12), 27,821–27,847.

List of Figures

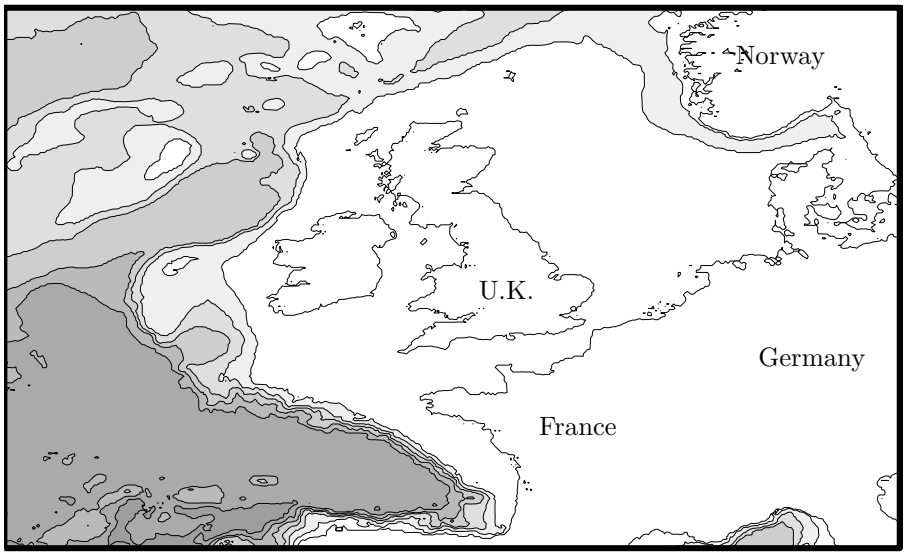

Fig. 1. The domain of interest, which extends from $20°W$ to $13°E$ and from $43°N$ to $63°N$. The filled isobaths ranges from $-6000\,m$ to $-200\,m$ by step of $1000\,m$. The continental shelf is visualized by the $-200\,m$ isobath.

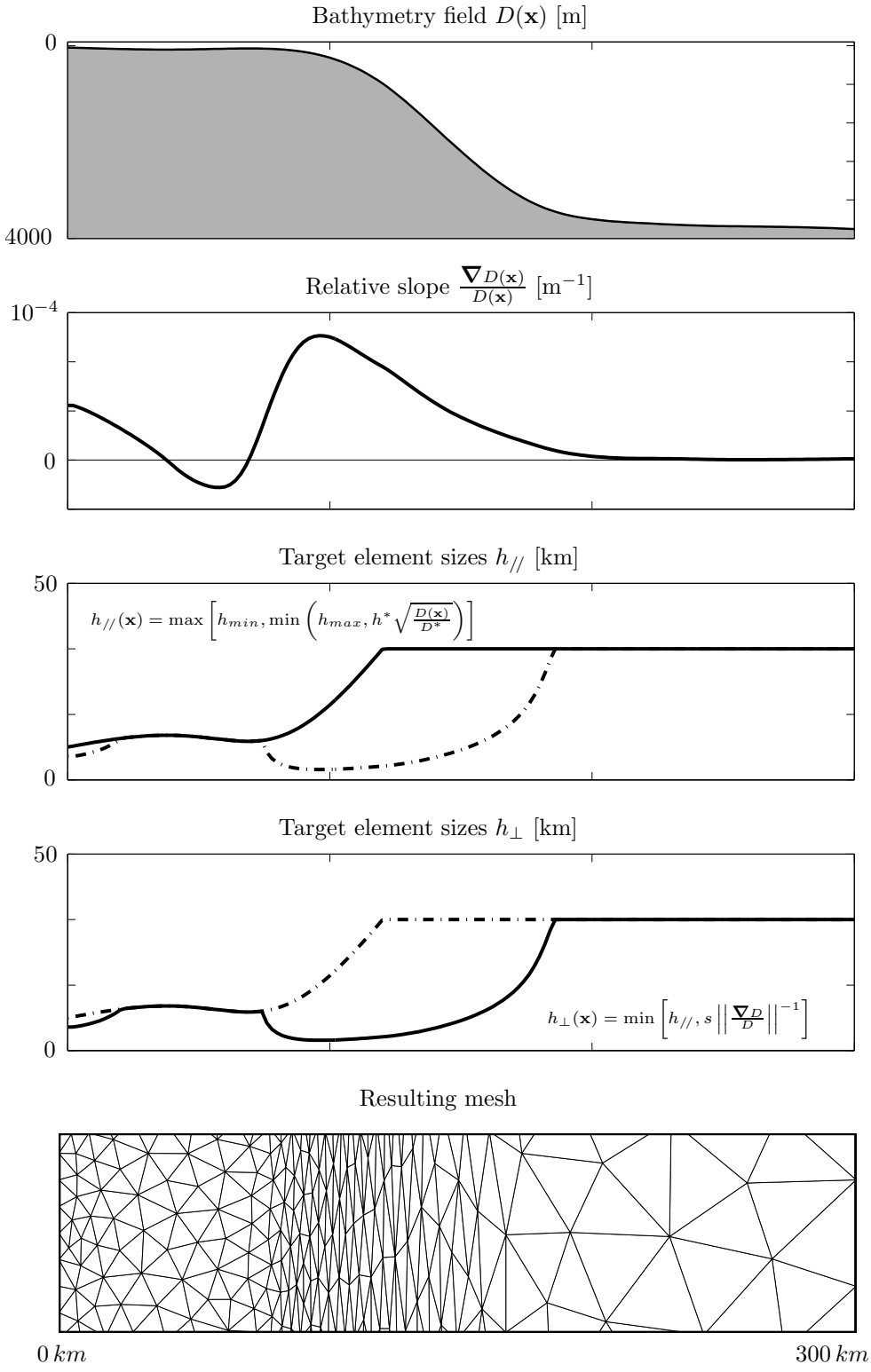

Fig. 2. Illustration of our anisotropic mesh refinement strategy for an idealised bathymetric profile including three regions that may be regarded as, from left to right, the shelf, the continental slope and the ocean. The strategy mixes requirements associated with the tidal wave propagation on the continental shelf and with the hydrostatic consistency condition in steep areas.

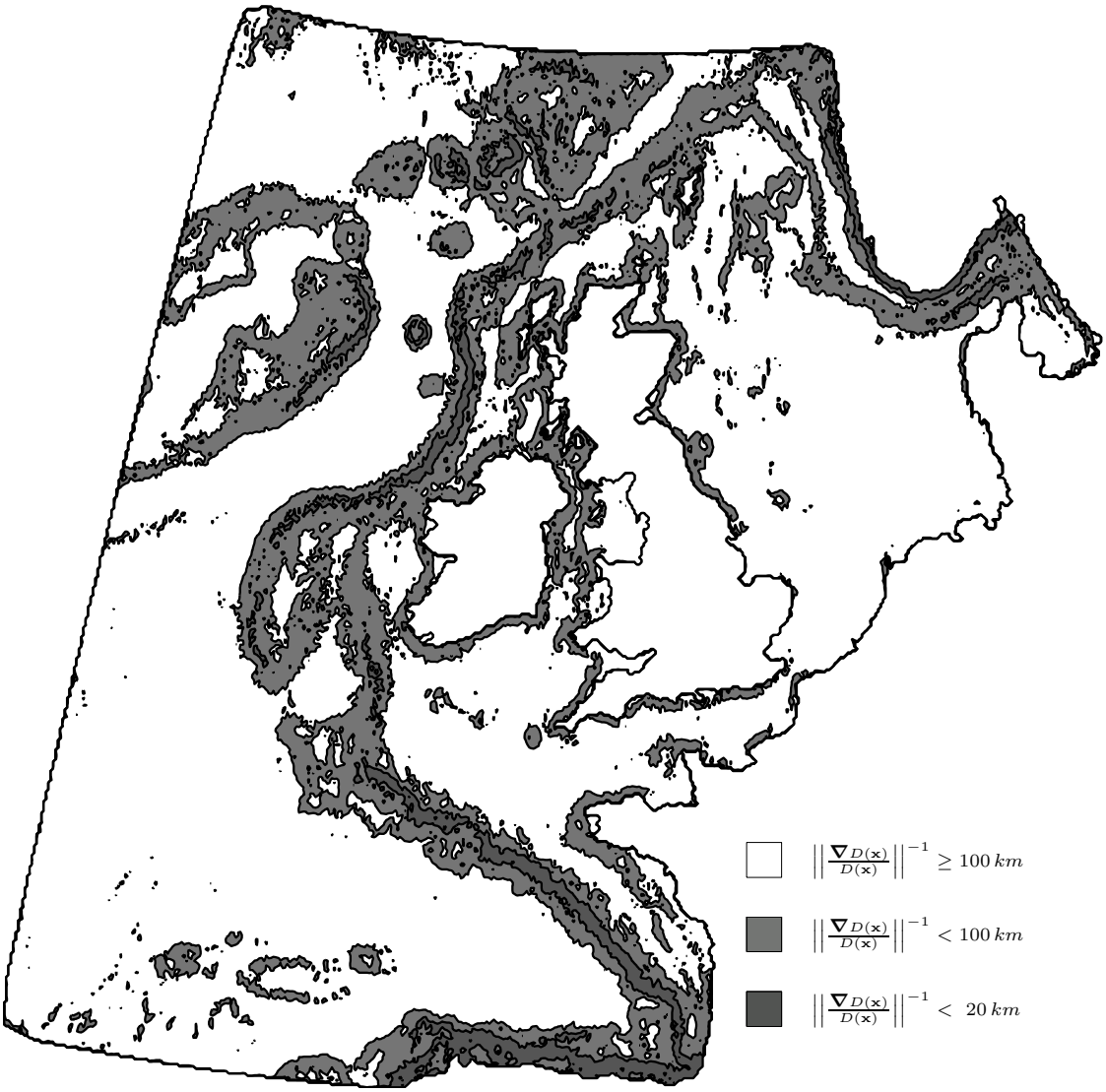

Fig. 3. The spatial distribution of the horizontal length scale $\left|\left|\frac{\nabla D(\mathbf{x})}{D(\mathbf{x})}\right|\right|^{-1}$. The regions where the latter is relatively small are those in which anisotropic elements are likely to be needed, i.e. the continental slope, coastal regions and seamounts.

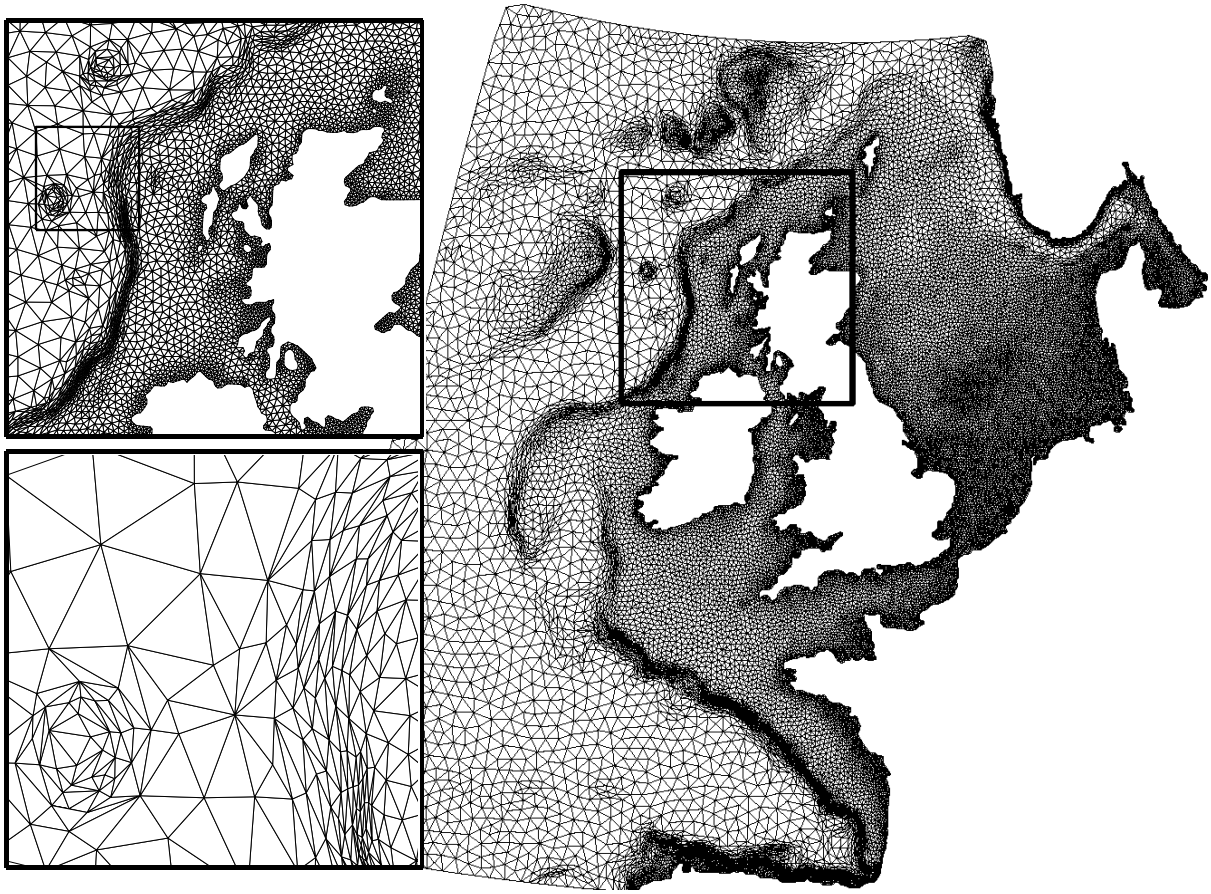

Fig. 4. A rather coarse mesh of the domain of interest with two recursive close-up views on the Hebridean shelf and the Anton Dohrn sea-mount.

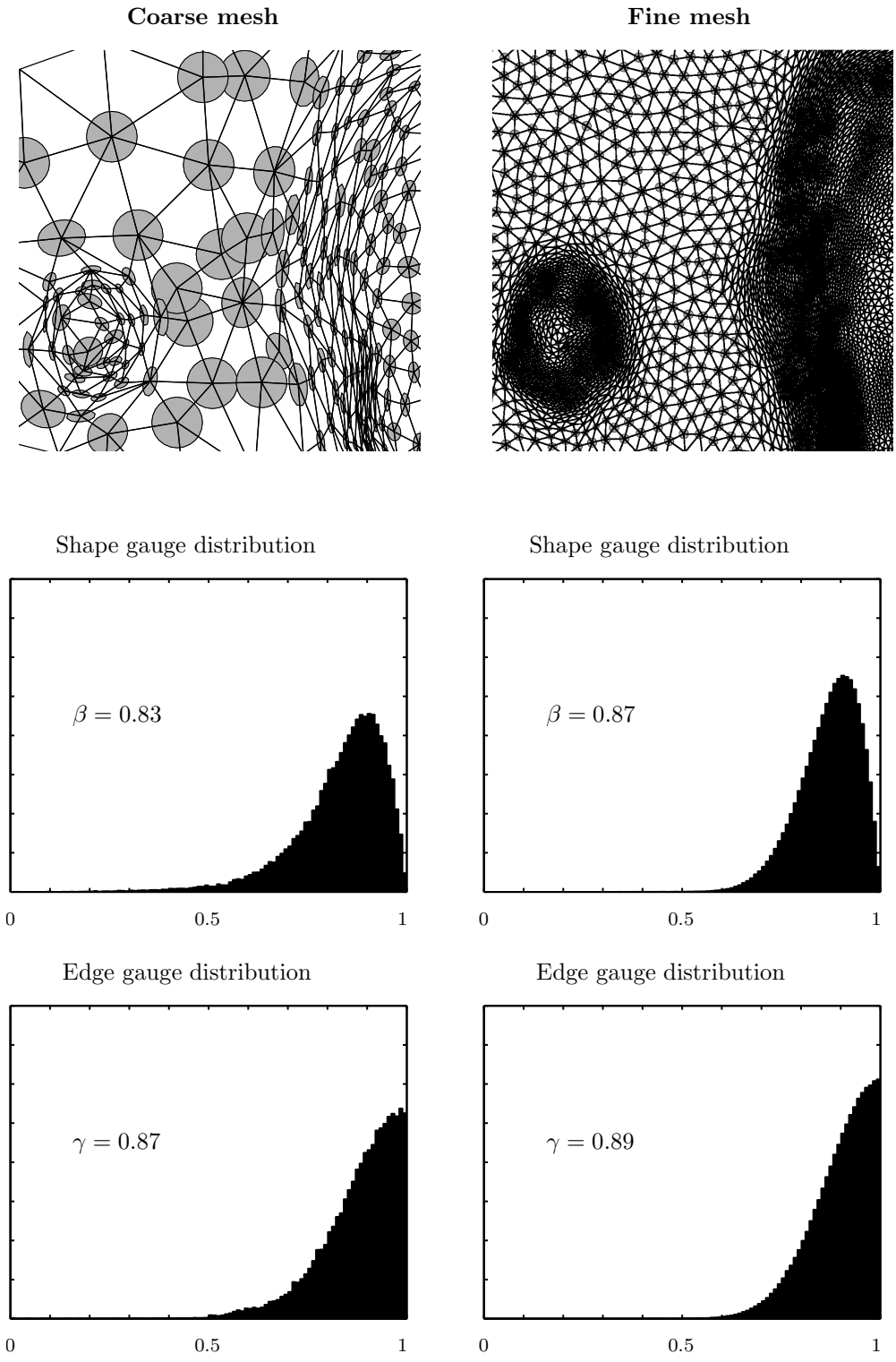

Fig. 5. Comparison between the length, the shape and the orientation of the ellipses and mesh elements to illustrate the way our mesh generator can fulfill the prescribed metric under quality constraints. Since the ellipse length is the half of the target element size, we may conclude that most discrepancies arise in areas of large element size variations. The normalized distribution of both quality gauges for the whole meshes.

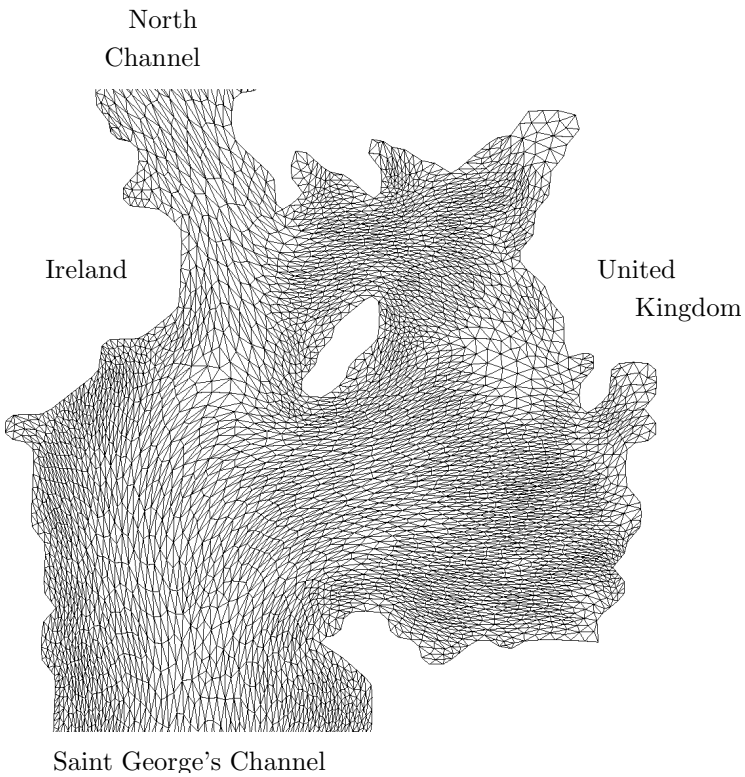

Fig. 6. A close-up view of a mesh in which the tidal ellipses are taken into account to introduce some anisotropy on the continental shelf. This may be an attractive improvement of our mesh refinement strategy in order to take into account the 'channel effect' that guides the flow through narrow passages as the North Channel or the Saint George's one.

	Coarse mesh	**Fine mesh**
D^*	25 m	10 m
h^*	6 km	0.5 km
s	0.3	0.05
h_{min}	6 km	0.5 km
h_{max}	38 km	5 km
# vertices	29 121	865 754
# elements	55 209	1 714 057
# edges	84 355	2 579 855
β	0.83	0.87
γ	0.87	0.89

Table 1
The values of our mesh refinement strategy parameters and the basic features of the corresponding meshes.